Journal of Materials Science and Chemical Engineering, 2025, 13(12), 97-122
https://www.scirp.org/journal/msce
ISSN Online: 2327-6053
ISSN Print: 2327-6045

Thermal and Viscous Performance in Finned Heat Pipes Heat Exchangers Using the Thermal Efficiency Method: IFHPHE versus AFHPHE

Élcio Nogueira, Quezia Manuela Gonçalvez Laurindo, Maria Victoria Cabrera Aguilera, Alvaro Pereira

Departamento de Mecânica e Energia (DME), Universidade do Estado do Rio de Janeiro-(FAT/UERJ), Resende, Brazil
Email: elcionogueira@uerj.br

How to cite this paper: Nogueira, É., Laurindo, Q.M.G., Aguilera, M.V.C. and Pereira, A. (2025) Thermal and Viscous Performance in Finned Heat Pipes Heat Exchangers Using the Thermal Efficiency Method: IFHPHE versus AFHPHE. *Journal of Materials Science and Chemical Engineering*, **13**, 97-122.
https://doi.org/10.4236/msce.2025.1312006

Received: November 25, 2025
Accepted: December 20, 2025
Published: December 23, 2025

Abstract

This work compares two heat exchangers that use finned heat tubes: a cross-flow finned tube heat exchanger with individual fins (IFHPHE) and an axially finned tube heat exchanger with parallel flow in the evaporator and counter-flow in the condenser (AFHPHE). The IFHPHE heat exchanger was designed and experimentally implemented to operate in small air conditioning systems with air flow rates in the range of 300 to 500 m^3/h. The AFHPHE heat exchanger is in the theoretical design phase and has the potential to be used in air conditioning systems for operating rooms of 60 m^3, with an air flow rate of 0.20 kg/s. The method used for theoretical comparisons between heat exchangers is the thermal efficiency method, and the main quantities obtained for comparison are velocities, Nusselt numbers, thermal effectiveness, air outlet temperatures, pressure drops, and Bejan numbers in the evaporator, condenser, and heat exchanger. The working fluid used is refrigerant R404a. The saturation temperature is 17.0˚C, with a fixed number of fins for both heat exchangers, equal to 30 fins, and 49 heat pipes as standard. Comparisons demonstrate superior thermal performance and very similar viscous performance when AFHPHE is compared to IFHPHE with 30 fins. When the simulations consider 70 fins for the IFHPHE, the thermal performances are very close to those of the AFHPHE with 30 fins. However, in this last case, with 70 fins, the viscous performance is very high and should not be implemented in real-world situations.

Keywords

Heat Exchangers, Individually Finned Heat Tubes, Axially Finned Heat Tubes (AFHPHE), Thermal Efficiency Method, Viscous Performance, Bejan Number

1. Introduction

Two finned heat tube heat exchangers are compared. One of the heat exchangers in question, called the Individually Finned Heat Tube Heat Exchanger (IFHPHE), was designed and implemented experimentally [1]. The second heat exchanger, called the Axially Finned Heat Tube Heat Exchanger (AFHPHE), was developed and implemented theoretically using the Thermal Efficiency Method [2]. Both heat exchangers were designed for use in small air conditioning systems, with great potential for use in operating rooms.

Górecki, G. *et al.* [1] are dedicated to the modeling, design and experimental study of a heat tube heat exchanger used as a recuperator in small air conditioning systems (air flow ≈ 300 - 500 m^3/h), composed of heat tubes with individual fins (IFHPHE). The designed heat exchanger was built and tested on the experimental bench. The refrigerant R404A was chosen as the working fluid based on preliminary results. The heat exchanger implementation contains 20 rows of finned heat tubes in a staggered arrangement, with 49 heat tubes. The configuration was optimized to maximize efficiency (up to 66%) and minimize pressure drop (less than 150 Pa), and the experimental data showed a good level of agreement with the model—relative difference less than 10%.

Nogueira, É. *et al.* [2] implement a theoretical model with axially finned thermosiphons, aiming at thermal comfort in air conditioning systems. The idealized configuration uses as a reference a heat exchanger with a radial finned heat pipe, whose theoretical and experimental analysis is already well established [1]. They apply the thermal efficiency method to determine thermal quantities, and the second law of thermodynamics to determine thermal and viscous irreversibilities. They present numerical and graphical results for the physical quantities of velocities, Reynolds numbers, Nusselt numbers, convection heat transfer coefficients, number of thermal units, heat transfer rates, friction factors, pressure drops and Bejan number. The results demonstrate the expected physical consistency for all the quantities analyzed. They conclude that the developed model presents promising results and should be used in the experimental implementation of an air conditioning system for operating rooms.

Nandy Putra, Trisno Anggoro, and Adi Winarta [3] state that hospital heating, ventilation and air conditioning systems consume large amounts of energy. They propose the use of high-pressure water heat exchangers (HPHEs) as an alternative to minimize consumption. They conduct experiments to investigate the performance of HPHEs consisting of several heat pipes with water as the working fluid, arranged in rows. They experimentally determined the effect of inlet air temperature, the effect of air velocity and the influence of the number of rows of heat pipes. They obtained results using six rows of high-pressure water heat exchangers (HPHEs), an air velocity of 1 m/s and an evaporator inlet air temperature of 45˚C. They demonstrate that the total energy consumption in the implemented air conditioning system, based on the annual heat recovery forecast for 8 h/day and 365 days/year, decreases significantly from 0.6 to 4.1 GJ/year.

Ragil Sukarno *et al.* [4] cite specific requirements related to thermal comfort that made it necessary to create heat recovery systems using a heat pipe exchanger (HPHE). They built an experimental apparatus with three, six, and nine rows of heat pipes, arranged in a staggered configuration. They use the ε-NTU method to predict the effectiveness, the evaporator-side outlet temperature, and the energy recovery of the HPHE. They find that the energy recovery of the HPHE increased with the number of rows, the air inlet temperature, and the air velocity in the evaporator section. They conclude that the ε-NTU method can be used for the analysis of heat recovery systems that apply air conditioning systems with HPHE.

Imansyah Ibnu Hakim, Ragil Sukarno, and Nandy Putra [5] argue for the need to use heating, ventilation and air conditioning (HVAC) systems to reduce energy consumption in buildings. They present a study that aims to investigate the use of a U-shaped finned heat pipe heat exchanger (HPHE). They performed tests with single and double row configurations, arranged in eight heat pipes per row. The results show that the U-shaped heat pipe heat exchanger significantly affects the pre-cooling and reheating processes in the HVAC system. They state that the U-shaped heat pipe proved to be a viable solution for HVAC systems that require cooling for reheating.

Élcio Nogueira [6] applies the thermal efficiency method to the theoretical analysis of the thermal performance of a finned heat pipe heat exchanger (FHPHE), used as an auxiliary device to control the temperature and quality of air conditioning in operating rooms. The theoretical analysis performed is point-by-point and distributed, divided into three aspects: analysis of the evaporator section, analysis of the condenser section, and analysis of the heat exchanger in terms of overall performance. It uses a theoretical-experimental study, which uses the concept of thermal effectiveness (ε-NTU) as a comparison object, and demonstrates that the localized theoretical-experimental comparisons are consistent, and the absolute relative error for the overall heat transfer rate varies from 0.5% to 35% for the heat exchanger under analysis.

Élcio Nogueira [7] applies a theoretical procedure to determine the performance of an individually finned heat exchanger (IFHPHE) used in an air conditioning system. The relevant variables used to determine the results are the number of fins per heat tube and the number of heat tube rows. A theoretical-experimental comparison demonstrates that the applied localized model can be used as a comprehensive design and analysis tool for finned heat exchangers. Results obtained for the Bejan number, which relates thermal and viscous irreversibilities, show that fin numbers between 10 and 20 for 49 heat tubes provide a better cost-benefit ratio. The absolute percentage errors obtained between the theoretical and experimental values for the overall heat transfer rate and overall thermal efficiency range from 2.0% to 42.1%.

2. Methodology

Analytical solution using the Thermal Efficiency Method. A comparison was made between two specific types of finned heat exchangers. The theoretical for-

mulations are explained through the expressions and equations below. When there is a difference in formulation between the heat exchangers under analysis, the representation for AFHPHE will be shown in red, and for IFHPHE in black.

The Thermal Efficiency Method, so named by Élcio Nogueira [8], based on work published by Ahamad Fakheri [9], has been used in many theoretical versus experimental comparisons in recent years. Thermal efficiency, obtained through an analogy of the thermal performance of finned systems, is the main quantity used to determine the thermal performance of heat exchangers. The effectiveness and rate of heat transfer of the heat exchanger are obtained from the thermal efficiency, since this physical quantity, like thermal effectiveness, measures the potential associated with the heat exchanger. Low thermal efficiency means that the heat exchanger has exhausted all its capacity for exchange between fluids and, in this sense, shows a tendency opposite to thermal efficiency.

The refrigerant used in simulations and experimental theoretical comparisons is R404a, due to its good thermodynamic properties for heat transfer, making it efficient in refrigeration and air conditioning applications. R404a has low toxicity and is non-flammable; it is considered safe for use in closed systems; it operates in pressure ranges compatible with many heat exchanger designs, facilitating control and safety; it is compatible with materials commonly used in industrial refrigeration systems; and it is efficient in applications requiring low temperatures.

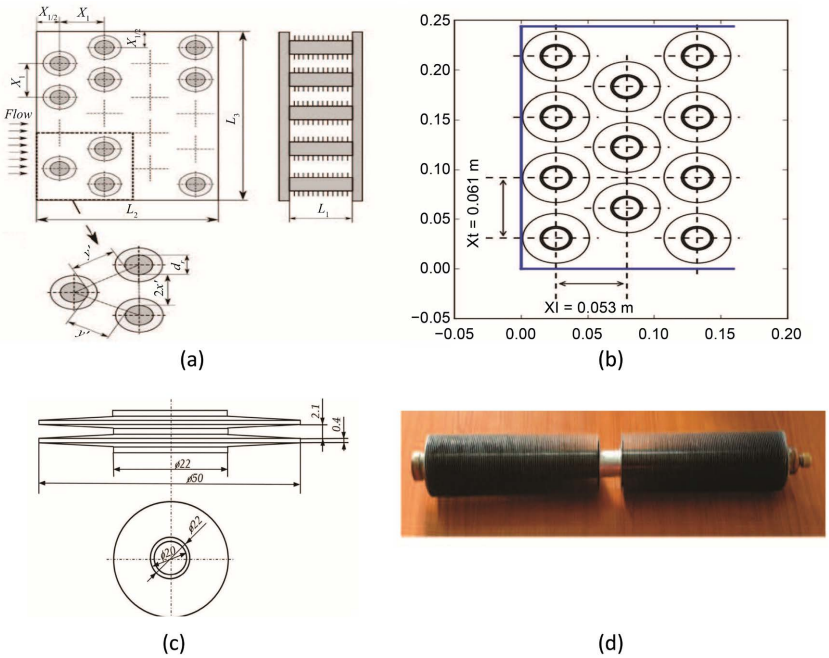

Figure 1. Geometric representation and design of Individually Finned Heat Pipe Heat Exchanger—IFHPHE.

Figures 1(a)-(d) above are part of the IFHPHE design project, reported through reference [1]. They represent the staggered configuration of the thermosiphons, the dimensions, the thermosiphon regions and the fins.

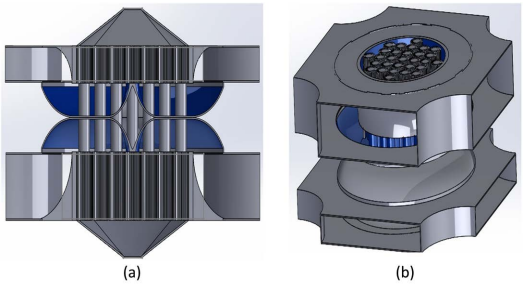

Figure 2. Initial design of AFHPHE.

Figures 2(a)-(b) above represent the initial design of the AFHPHE, with the thermosiphons, the evaporator regions, the adiabatic region, the condenser region and the 4 air outlet areas per region [2].

The analysis was divided into three aspects and regions of the device: evaporator, condenser, and heat exchanger. The analysis related to the evaporator is more complete and includes all the essential parameters so that the comparisons between the heat exchangers could be as complete as possible. The analyses related to the condenser and FHPHE present only the essential parameters so that a global analysis of the heat exchangers could be successfully concluded.

The saturation temperatures of the working fluid and inlets, in both heat exchangers, are the same.

$$T_{sat} = 17.0^{\circ}\text{C};\ T_{Evin} = 30.0^{\circ}\text{C};\ T_{Cdin} = 10.0^{\circ}\text{C} \tag{1}$$

The mass flow rates in the evaporator and condenser are within the range specified below.

$$0.12\,\text{kg/s} \le \dot{m}_{air} \le 0.20\,\text{kg/s} \tag{2}$$

The number of heat pipes and the number of fins per heat pipe are defined by the expressions below.

$$N_{HP} = 49\ default;\ N_{Fin} = 30\ default \tag{3}$$

where, by AFHPHE:

$$N_R = \sqrt{N_{HPb}},\ N_{HPb} = 16\ heat\ pipes \tag{4}$$

$$N_{HPR} = N_R + \left(N_R + 1.0\right) \tag{5}$$

N_{HPR} is the number of heat pipes per row.

Finally, the number of heat pipes is represented by Equation (6).

$$N_{HP} = N_{HPR} * \left(N_R + 1.0\right) + N_R \tag{6}$$

The tubes and fins are made of aluminum, and the thermal conductivity adopted is represented by the expression below.

$$k_W = 235\ \text{W/(m K)} \tag{7}$$

The internal and external diameters are different for both heat exchangers.

$$D_{int} = 50.08\ \text{mm};\ D_{ext} = 50.973\ \text{mm};\ D_{int} = 20.0\ \text{mm};\ D_{ext} = 22.0\ \text{mm} \tag{8}$$

The lengths associated with the evaporator and condenser are different for both heat exchangers.

$$L_{ev} = 220.0 \text{ mm};\ L_{cd} = 120.0 \text{ mm};\ L_{ev} = 250.0 \text{ mm};\ L_{cd} = 250.0 \text{ mm} \quad (9)$$

The fin thickness and fin height are defined by the expressions below.

$$T_{Fin} = 4.0 \text{ mm};\ \Delta H_{Fin} = 18.0 \text{ mm};\ T_{Fin} = 0.8 \text{ mm} \quad (10)$$

The space between fins is obtained using the following expressions:

$$Sp_{Fin} = \left(P_{HP} - N_{Fin} * T_{Fin}\right) / \left(N_{Fin} + 1.0\right);\ Sp_{Fin} = 2.5 \text{ mm } \textit{by definition} \quad (11)$$

where,

$$P_{HP} = \pi D_{ext} \quad (12)$$

The shell diameter and channel width are expressed using the formulas below.

$$D_{Shell} = 9.0 * \left(D_{ext} + 2 * \Delta H_{Fin}\right) \text{mm};\ W_{HE} = 200.0 \text{ mm } \textit{by definition} \quad (13)$$

The air intake area is expressed by:

$$A_{air} = \left(\pi D_{Shell}^2\right) / 4 \quad (14)$$

The air passage area is obtained using the following expression:

$$Asec_{air} = A_{air} - \left(NHP * \pi D_{ext}^2 / 4\right) - \left(Ntot_{Fin} * \Delta H_{Fin} * T_{Fin}\right) \quad (15)$$

$$Asec_{air} = \left(\dot{m}_{air} * Dh_{Ev}\right) / \left(\mathrm{Re}_{air} * \mu_{air}\right) \quad (16)$$

where,

$$Ntot_{Fin} = NHP * N_{Fin} \quad (17)$$

2.1. Equations for Evaporator

The hydraulic diameter in the evaporator is expressed by:

$$Dh_{Ev} = \left(4 * Asec_{air}\right) / Ph_{Ev};\ Dh_{Ev} = \left(4 * W_{HE}\right) / \left[2 * \left(W_{HE} + LEv_{effec}\right)\right] \quad (18)$$

where,

$$Ph_{Ev} = NHP * P_{HP} + Ntot_{Fin} * \left(2 * \Delta H_{Fin} + T_{Fin}\right);\ LEv_{effec} = L_{Ev} - N_{Fin} * \left(T_{Fin} + Sp_{Fin}\right) \quad (19)$$

The heat exchange area between the fluids in the evaporator depends on two areas, namely:

$$A_{TotalEv} = Atr_{Fin} + Atr_{NHP} \quad (20)$$

where,

$$Atr_{Fin} = L_{Ev} * NHP * \left(2 * \Delta H_{Fin} + T_{Fin}\right);\ Atr_{Fin} = N_{Fin} * NHP * \pi * \left(D_{extFin}^2 - D_{intFin}^2\right) / 4 \quad (21)$$

The boiling coefficient is obtained through the Gupta and Varshney correlation [10], for both heat exchangers.

$$h_{boil} = 1.39 * \left(k_{water} / l_*\right) * \left[Heat_{Flux} * \rho_{water} * Cp_{water} * l_* / \left(\rho_l * h_{lv} * k_{water}\right)\right]^{0.7} * \left(\rho_l / \rho_v\right)^{0.21} * \left(\mu_{water} * Cp_{water} / k_{water}\right)^{(-0.21)} \quad (22)$$

Heat flux is determined from the Pioro correlation [11] [12]:

$$Heat_{Flux} = \mu_{Water} * h_{lv} * l_* * \left(1.0/C_{sf}\right)^{0.33} * \left(Pr_{Water}\right)^{1.0/0.33} * \left(Cp_{Water} * \left(\Delta T_{Evsat}\right)/h_{lv}\right)^{1.0/0.33} \quad (23)$$

where,

$$l_* = \left[\sigma_{Water}/\left(g*\left(\rho_l - \rho_v\right)\right)\right]^{(1/2)} \quad (24)$$

The saturation temperature difference across the evaporator is represented by Equation (25).

$$\Delta T_{Evsat} = T_{airin} - T_{sat} \quad (25)$$

The Nusselt number associated with air is represented by the equations below.

$$Nu_{airEv} = 0.696 * Re_{AirEv}^{0.5} * Pr_{air}^{0.36} * \left[Pr_{air}/\left(5.0 * Pr_{air}\right)\right]^{0.25} \quad (26)$$

$$Nu_{airEv} = 0.1387 * Re_{dr}^{0.718} * Pr_{air}^{(1/3)} \left(Sp_{Fin}/\left(Dext_{Fin} - Dint_{Fin}\right)\right)^{0.296} \quad (27)$$

where,

$$Dext_{Fin} = 50.0 \text{ mm and } Dint_{Fin} = D_{ext} \quad (28)$$

and,

$$Re_{AirEv} = \left(4.0 * \dot{m}_{air}\right)/\left(\pi * Dh_{Ev} * \mu_{air}\right);\ Re_{dr} = \left(Vair_{max}\right)/v_{air};\ Sp_{Fin} = 2.5 \text{ mm } \textit{by definition} \quad (29)$$

The heat transfer coefficient by air convection in the evaporator is obtained by:

$$h_{Ev} = Nu_{airEv} * k_{air}/\text{Dext} \quad (30)$$

The application of the concept of "Fin Analogy", conceived by Fakheri [8], leads us to define the following parameters:

$$mL_{EvFin} = \sqrt{2 * h_{Ev}/\left(k_{Fin} * t_{Fin}\right)} * P_{hEv} \quad (31)$$

$$\eta_{EvFin} = Tanh\left(mL_{EvFin}\right)/mL_{EvFin} \quad (32)$$

The fin efficiency for the evaporator section is defined through Equation (32) by η_{EvFin} [8] [9]. This quantity is fundamental in theoretical and experimental studies on the thermal performance of fins and is widely used in finned systems analyzed by Élcio Nogueira [13].

$$\beta_{\_Ev} = A_{\_trFin}/A_{totEv} \quad (33)$$

$$\eta'_{EvFin} = \beta_{Ev}\eta_{EvFin} + \left(1 - \beta_{Ev}\right) \quad (34)$$

The global heat transfer coefficient associated with air in the Evaporator, Uo_{Ev}, is given by Equation (35).

$$Uo_{Ev} = 1/\left[1/h_{boil} + \left(D_{ext} - D_{int}\right)/kW + 1/\left(\eta'_{EvFin} h_{Ev}\right)\right] \quad (35)$$

The heat capacity of the air in the Evaporator is given by C_{Air}.

$$C_{Air} = \dot{m}_{air} Cp_{air} \quad (36)$$

The number of thermal units associated with air in the evaporator, NTU_{Ev}, is given by Equation (37).

$$NTU_{Ev} = \left(Uo_{Ev} * A_{totEv}\right) / C_{Ev};\ C_{Ev} = C_{air} \tag{37}$$

The dimensionless number, called "fin analogy," Fa_{Ev} is represented by Equation (35) as defined by Ahamad Fakheri [8] and reported by Nogueira, É. [9].

$$Fa_{Ev} = NTU_{Ev} / 2.0 \ \textit{for parallel flow} \tag{38}$$

The thermal efficiency associated with the evaporator is η_{TEv} [8] [9].

$$\eta_{TEv} = \left(Tanh\left(Fa_{eV}\right)\right) / \left(Fa_{eV}\right) \tag{39}$$

$$\varepsilon_{TEv} = 1 / \left[1 / \left(\eta_{TEv}\ NTU_{Ev}\right) + 1/2\right] \tag{40}$$

The thermal effectiveness associated with the heat evaporator is ε_{TEv}.

The heat transfer rate between the air and the heat pipe in the evaporating region $\dot{Q}_{Ev}$ is given by Equation (41).

$$\dot{Q}_{Ev} = \left(C_{Ev} \Delta T_{Evsat}\right) / \left[1 / \left(\eta_{TEv}\ NTU_{Ev}\right) + 1/2\right] \tag{41}$$

After passing through the evaporator, the outlet air temperature is represented by the equation below.

$$T_{airout} = T_{airin} - \dot{Q}_{Ev} / C_{Ev} \tag{42}$$

$$Irrev_{TEv} = ln\left(T_{airin} / T_{airout}\right) \tag{43}$$

$Irrev_{TEv}$ is the thermal irreversibility in the evaporator.

The rate of thermal entropy generation is represented by $\dot{S}gen_{TEv}$.

$$\dot{S}gen_{TEv} = Irrev_{TEv} * C_{Ev} \tag{44}$$

The pressure drop across the evaporator is represented by Equation (45).

$$\Delta p_{Ev} = Fric_{Ev} * \left(L_{Ev} / D_{hEv}\right) * \left[\left(\rho_{Air} * V_{AirEv}^2\right) / 2\right];\ \Delta p_{Ev} = 2 f_{Ev} N_{rows} \rho_{air} Vair_{\max} \tag{45}$$

where, $Fric_{Ev}$ and f_{Ev} are the friction factors in the evaporator.

$$Fric_{Ev} = 0.31 / Re_{AirEv}^{0.25};\ f_{Ev} = 0.7465 * Re_{dr}^{(-0.316)} \left(X_t / dr\right)^{(-0.927)} \tag{46}$$

$$X_t = Dext_{Fin} \tag{47}$$

Viscous irreversibility in the evaporator is obtained using the equation below.

$$Irrev_{VEv} = \ln\left(P_{2Ev} / P_{1Ev}\right) \tag{48}$$

where,

$$P_{1Ev} = P_{2Ev} + \Delta p_{Ev} \text{ and } P_{2Ev} = P_{atm} \tag{49}$$

The rate of viscous entropy generation is represented by Equation (47).

$$\dot{S}gen_{VEv} = Irrev_{VEv} * C_{Ev} \tag{50}$$

The Bejan number [14] in the evaporator is represented by Equation (51).

$$Be_{Ev} = \dot{S}gen_{TEv} / \left(\dot{S}gen_{TEv} + \dot{S}gen_{VEv}\right) \tag{51}$$

2.2. Equations for Condenser

The heat exchange area of the heat pipes in the condenser is represented by Equation (52).

$$A_{trCd} = L_{Cond} * N_{HP} * \left(P_{HP} - N_{Fin} * T_{Fin}\right) \tag{52}$$

The heat exchange area in the condenser is represented by Equation (53).

$$A_{totCd} = A_{trFin} + A_{trCd} \tag{53}$$

The Reynolds number associated with the air flow inside the condenser is represented by Equation (54).

$$\mathrm{Re}_{AirCd} = \left(4.0 * \dot{m}_{air}\right) / \left(\pi * D_{hCd} * \mu_{air}\right) \tag{54}$$

The air velocity inside the condenser is represented by Equation (52).

$$V_{AirCd} = \left(Re_{AirCd} * \mu_{air}\right) / D_{hCd} \tag{55}$$

$$D_{hCd} = 4 * Asec_{air} / Ph_{Cd}\ ;\ Dh_{Cd} = \left(4 * WHELCd_{effec}\right) / \left[2 * \left(WHE + LCd_{effec}\right)\right] \tag{56}$$

$$\begin{aligned} Ph_{Cd} &= NHP * P_{HP} + Ntot_{Fin} * \left(2 * \Delta H_{Fin} + T_{Fin}\right); \\ LCd_{defffec} &= L_{Cd} - N_{Fin} * \left(T_{Fin} + Sp_{Fin}\right) \end{aligned} \tag{57}$$

The saturation temperature difference across the condenser is represented by Equation (58).

$$\Delta T_{Cdsat} = T_{sat} - T_{airin} \tag{58}$$

The condensation coefficient in the condenser is represented by Equation (59).

$$h_{Cond} = 0.943 * \left[\left(\rho_l * \left(\rho_l - \rho_v\right) * h_{lv} * g * k_{water}^3\right) / \left(\mu_{water} * L_{Cd} * \Delta T_{Cdsat}\right)\right]^{1/4} \tag{59}$$

The Nusselt number associated with the air in the condenser is represented by Equation (60).

$$\begin{aligned} Nu_{airCd} &= 0.696 * \mathrm{Re}_{AirCd}^{0.5} * \mathrm{Pr}_{air}^{0.36} * \left[\mathrm{Pr}_{air} / \left(5.0 * \mathrm{Pr}_{air}\right)\right]^{0.25}; \\ Nu_{airCd} &= 0.1387 * \mathrm{Re}_{dr}^{0.718} * \mathrm{Pr}_{air}^{(1/3)} \left(Sp_{Fin} / \left(Dext_{Fin} - D\mathrm{int}_{Fin}\right)\right)^{0.296} \end{aligned} \tag{60}$$

The condensation transfer coefficient in the heat pipe is provided by h_{Cond}, as reported in [9].

$$h_{Cd} = Nu_{airCd} * k_{air} / \mathrm{Dext} \tag{61}$$

The application of the concept of "Aleta Analogy", conceived by Fakheri [9] leads us to define the following parameters:

$$mL_{CdFin} = \sqrt{2 * h_{Cd} / \left(k_{Fin} * t_{Fin}\right)} * P_{hCd} \tag{62}$$

$$\eta_{CdFin} = \mathrm{Tanh}\left(mL_{CdFin}\right) / mL_{CdFin} \tag{63}$$

The fin efficiency for the condenser section is defined through Equation (63) by η_{CdFin}.

$$\beta_{Cd} = A_{\_trFin} / A_{totEv} \tag{64}$$

$$\eta'_{CdFin} = \beta_{Cd}\eta_{CdFin} + (1-\beta_{Cd}) \tag{65}$$

The efficiency associated with the set of fins in the condenser, weighted by the area of change of the fins η'_{CdFin}, is represented through Equation (65).

$$Uo_{CD} = 1/\left[1/h_{boil} + (D_{ext} - D_{\text{int}})/kW + 1/(\eta'_{CdFin}h_{Cd})\right] \tag{66}$$

The global heat transfer coefficient associated with air in the condenser, Uo_{Cd}, is given by Equation (66).

$$C_{Air} = \dot{m}_{air}Cp_{air} \tag{67}$$

The heat capacity of the air in the condenser, C_{Air}, is given by Equation (67).

$$C_{Cd} = C_{air} \tag{68}$$

$$NTU_{Cd} = (Uo_{Cd} * A_{totCd})/C_{Cd};\ C_{Cd} = C_{air} \tag{69}$$

The number of thermal units associated with air in the condenser, NTU_{Cd}, is given by Equation (69).

$$Fa_{Cd} = NTU_{Cd}/2.0 \text{ for counter flow} \tag{70}$$

The dimensionless number, called "fin analogy," Fa_{Cd} is represented by Equation (70) as defined by Ahamad Fakheri [9] and reported by Nogueira, É. [8] [10].

$$\eta_{TCd} = (\text{Tanh}(Fa_{Cd}))/(Fa_{Cd}) \tag{71}$$

The thermal efficiency associated with the condenser is η_{TCd}.

$$\varepsilon_{TCd} = 1/\left[1/(\eta_{TCd}\ NTU_{Cd}) + 1/2\right] \tag{72}$$

The thermal effectiveness associated with the condenser is ε_{TCd}.

$$\dot{Q}_{Cd} = (C_{Cd}\Delta T_{Cdsat})/\left[1/(\eta_{TCd}\ NTU_{Cd}) + 1/2\right] \tag{73}$$

The heat transfer rate between the air and the heat pipe in the condenser region $\dot{Q}_{Cd}$ is given by Equation (73).

$$T_{airout} = \dot{Q}_{Cd}/C_{Cd} + T_{airin} \tag{74}$$

After passing through the condenser (heat recovery), the outlet air temperature is represented through Equation (74).

Thermal irreversibility in the condenser is obtained using Equation (75) below.

$$Irrev_{TCd} = \ln(T_{airin}/T_{airout}) \tag{75}$$

The rate of thermal entropy generation in the condenser is represented by Equation (76).

$$\dot{S}gen_{TCd} = Irrev_{TCd} * C_{Cd} \tag{76}$$

$$Fric_{Cd} = 0.31/\text{Re}_{AirCd}^{0.25};\ f_{Cd} = 0.7465 * \text{Re}_{dr}^{(-0.316)}(X_t/dr)^{(-0.927)} \tag{77}$$

The friction factor in the condenser is represented by Equation (77).

$$\Delta p_{Cd} = Fric_{Cd} * (L_{Cd}/D_{hCd}) * \left[(\rho_{Air} * V_{AirCd}^2)/2\right];\ \Delta p_{Cd} = 2 f_{Cd} N_{rows} \rho_{air} Vair_{\max} \tag{78}$$

The pressure drop across the condenser is represented by Equation (78).

The pressure at the evaporator inlet is represented by Equation (79).

$$P_{1Cd} = P_{2Cd} + \Delta p_{Cd} \tag{79}$$

By definition:

$$P_{2Cd} = P_{atm} \tag{80}$$

Viscous irreversibility in the condenser is obtained using Equation (81) below.

$$Irrev_{VCd} = \ln\left(P_{2Cd} / P_{1Cd}\right) \tag{81}$$

The rate of viscous entropy generation in the condenser is represented by Equation (82).

$$\dot{S}gen_{VCd} = Irrev_{VCd} * C_{Cd} \tag{82}$$

The Bejan number in the capacitor is represented by Equation (83).

$$Be_{Cd} = \dot{S}gen_{TCd} \Big/ \left(\dot{S}gen_{TCd} + \dot{S}gen_{VCd}\right) \tag{83}$$

2.3. Equations for Finned Heat Pipe Heat Exchanger—FHPHE

The theoretical method for obtaining the equations below, valid for the heat exchanger, called the localized method, uses the values obtained individually in the evaporator and condenser, according to the procedure recommended in references [6] [7].

$$\dot{Q}_{FHPHE} = \dot{Q}_{Ev} + \dot{Q}_{Cd} \tag{84}$$

$$\dot{Q}_{\max} = C_{\min}\left(T_{Evin} - T_{Cdout}\right) \tag{85}$$

$$\varepsilon_{FHPHE} = \dot{Q}_{FHPHE} \Big/ \dot{Q}_{\max} \tag{86}$$

$$\Delta p_{FHPHE} = \Delta p_{Ev} + \Delta p_{Cd} \tag{87}$$

$$\sigma_{THPHE} = \sigma_{TEv} + \sigma_{TCd} \tag{88}$$

$$\sigma_{fHPHE} = \sigma_{fEv} + \sigma_{fCd} \tag{89}$$

$$Be_{HPHE} = \sigma_{THPHE} \Big/ \left(\sigma_{THPHE} + \sigma_{fHPHE}\right) \tag{90}$$

Be_{HPHE} is the thermodynamic Bejan number associated with the heat exchanger.

3. Results and Discussion

This section presents results obtained through theoretical simulations and discusses their relevance. The main objective is to compare the thermal and viscous performances of the heat exchangers under analysis.

Comparisons are made for the results in the evaporator, condenser, and heat exchanger. The overall results obtained for the heat exchangers demonstrate that the localized analysis is consistent, since theoretical results can be compared with experimental results obtained for the IFHPHE.

The standard parameters for both heat exchangers under analysis are saturation temperature of the working fluid (R404a) equal to 17.0˚C; mass flow rate variation

between 0.12 kg/s and 0.20 kg/s; number of fins equal to 30; inlet temperatures in the evaporator and condenser equal to 30.0˚C and 10.0˚C, respectively. In some situations, presented, the number of fins is defined as equal to 70 fins for the IFHPHE, with the objective of comparing performance in relation to the number of 30 fins.

3.1. Evaporator

Figure 3 shows velocity values as a function of air mass flow rate in the evaporator. The air velocity for the IFHPHE is approximately twice that of the AFHPHE. The difference in velocities can be justified by the configuration of the heat exchangers, since the IFHPHE has a staggered configuration and crossflow with the air, that is, perpendicular to the direction of the air, creating a barrier to it. In the case of the AFHPHE, the air enters the evaporator in the direction of the heat pipes, and the only barrier it encounters is the frontal areas of the pipes and fins. Although the AFHPHE has heat pipes with approximately twice the diameter, the air passage area is larger, resulting in lower velocity. When the number of fins is reduced from 30 to 0 (zero) in the IFHPHE, the velocity drops sharply, demonstrating the influence of the fins on the heat exchanger's performance. Featured are the 49 finned thermosiphons in a diametrically symmetrical configuration. This design allows for homogeneous air distribution within the heat pipe, contributing to less viscous heat dissipation.

Figure 4 presents the result for the Nusselt number. Since the Nusselt number strongly depends on the Reynolds number, it is expected that IFHPHE will show a higher value for the Nusselt number compared to AFHPHE. The relationship between the Nusselt numbers is almost the same as that presented by the velocities, approximately double.

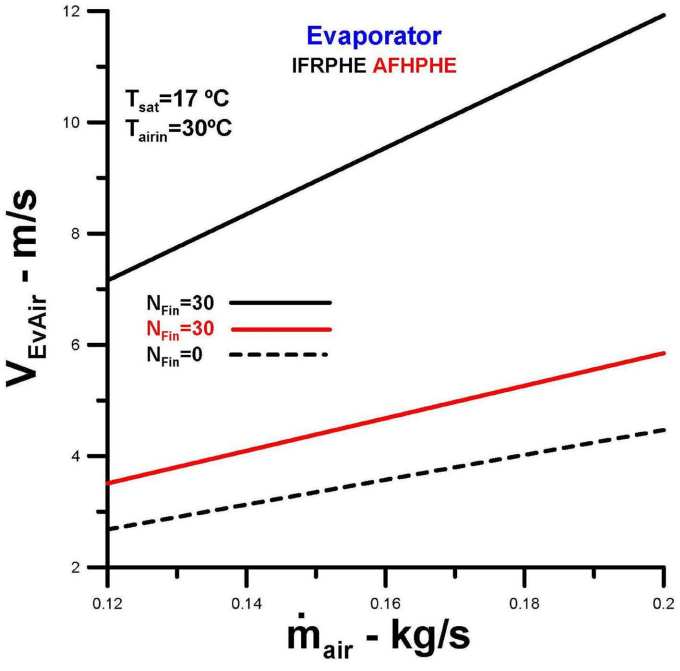

Figure 3. Air velocity in the evaporator.

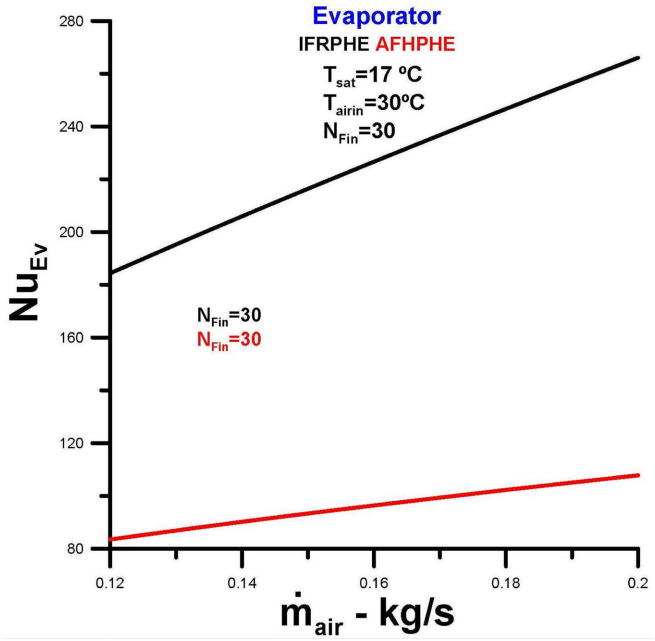

Figure 4. Nusselt number in the evaporator.

Figure 5 presents the result for the heat exchange areas. The heat exchange area of the IFHPHE is smaller than the heat exchange area of the AFHPHE despite having a greater length. The difference in this case is the diameter of the heat pipes, which is almost double the value. Even with a fin count of 70, the difference is significant and should be reflected in the thermal performance of both heat exchangers.

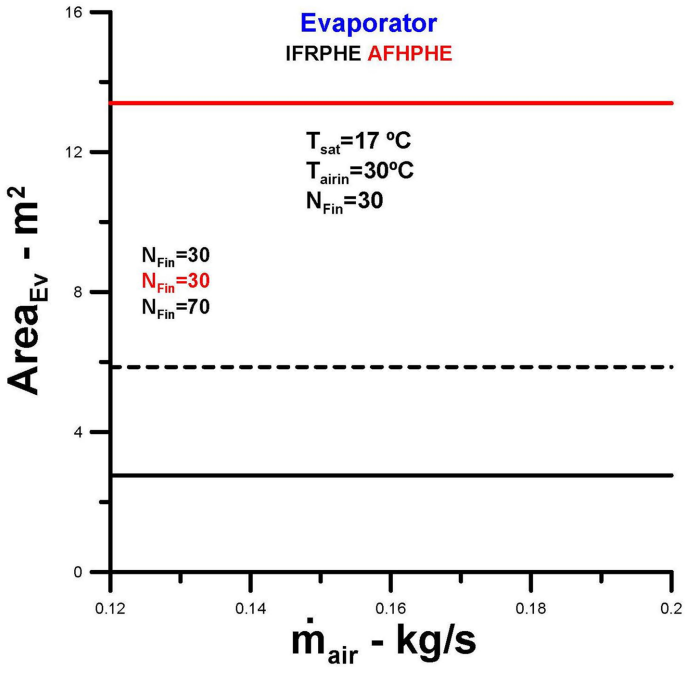

Figure 5. Heat exchange area.

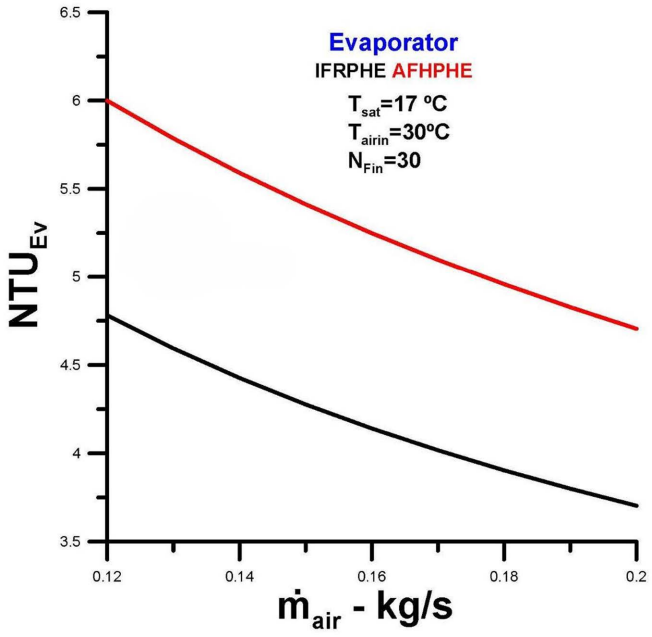

Figure 6. Number of thermal units—NTU.

The number of thermal units (NTU) of the AFHPHE, represented in Figure 6, surpasses the value obtained for the IFHPHE. This result can be explained by the larger heat exchange area of the AFHPHE. It is important to emphasize that although the Nusselt number is higher in the case of the IFHPHE, which reflects a higher value for the convection heat transfer coefficient, the predominant factor in determining the overall coefficient is the boiling coefficient, and this parameter is the same for both heat exchangers.

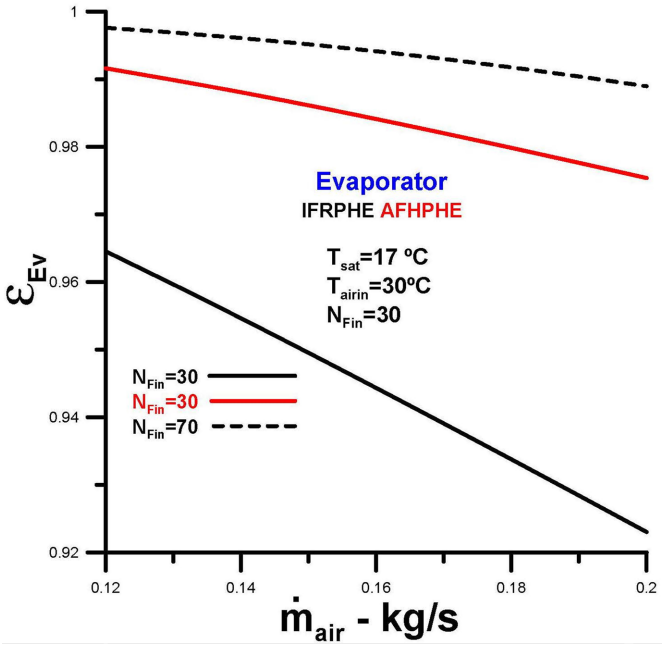

Figure 7. Effectiveness.

Values for effectiveness are represented in Figure 7. The values reflect what has already been evaluated and support the findings. The AFTHE has higher thermal effectiveness than the IFHPE when using 30 fins. However, the values presented for IFHPHE, in absolute terms, are not very different. It can be stated that in thermal terms, there is no significant difference, and this result should be reflected in the outlet temperatures. For comparison, analyzing the influence of the number of fins on the heat exchange area, it is found that the value presented for 70 fins in the IFHPHE is slightly higher than the value obtained by the AFTHE for 30 fins. There is no significant difference, once again, between the absolute values. However, the values demonstrate exceptional thermal performance for the AFTHE.

Outlet temperatures for both heat exchangers are shown in Figure 8. The results reflect and corroborate the evidence obtained and discussed previously. The outlet temperature of the air in the evaporator is lower for the AFHPHE compared to the IFHPHE for 30 fins. The difference increases with increasing flow rate, reflecting the observed values for thermal efficiency. When evaluating the influence of the number of fins, imposing 70 fins per heat pipe in the IFHPHE, a lower temperature value per flow rate is observed, as expected. Excellent thermal performance.

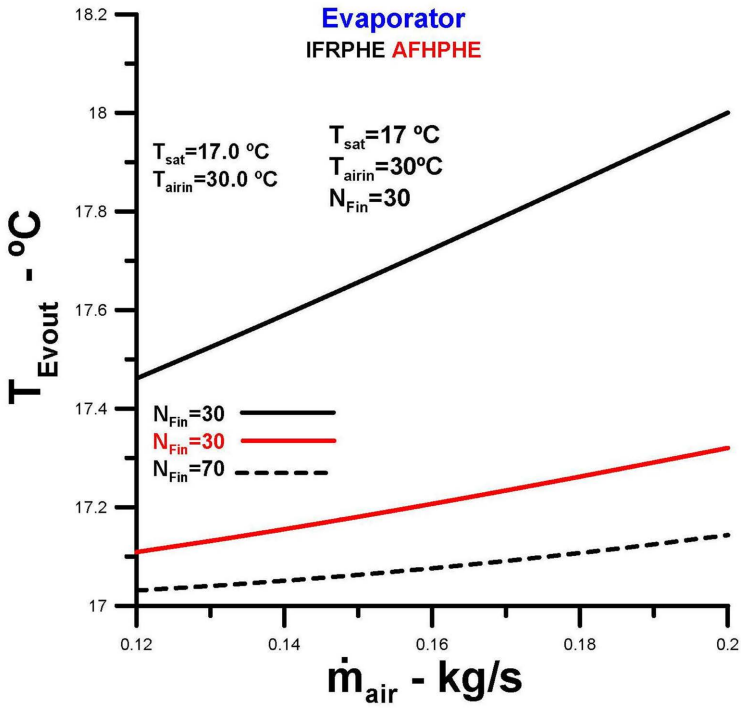

Figure 8. Outlet temperature.

Figure 9 presents the result of the pressure drop in the evaporator. The pressure drop in the evaporator is lower for the AFTHE heat exchanger with 30 fins. This result reflects a lower evaporator velocity. The difference decreases with increas-

ing flow rate. For an upper limit value of 0.20 kg/s, the pressure drops become closer, but the loss in the AFTHE is still lower. The higher-pressure drop observed by 70 fins in the IFHPHE reflects the greater number of fins. However, it should be noted that the pressure drop obtained for the AFTHE is only in the internal flow between the heat pipes and the shell. Pressure drop at the heat exchange outlet was not implemented, as this aspect is still under study and analysis. This important aspect will be discussed further in the analysis ahead and in the conclusion.

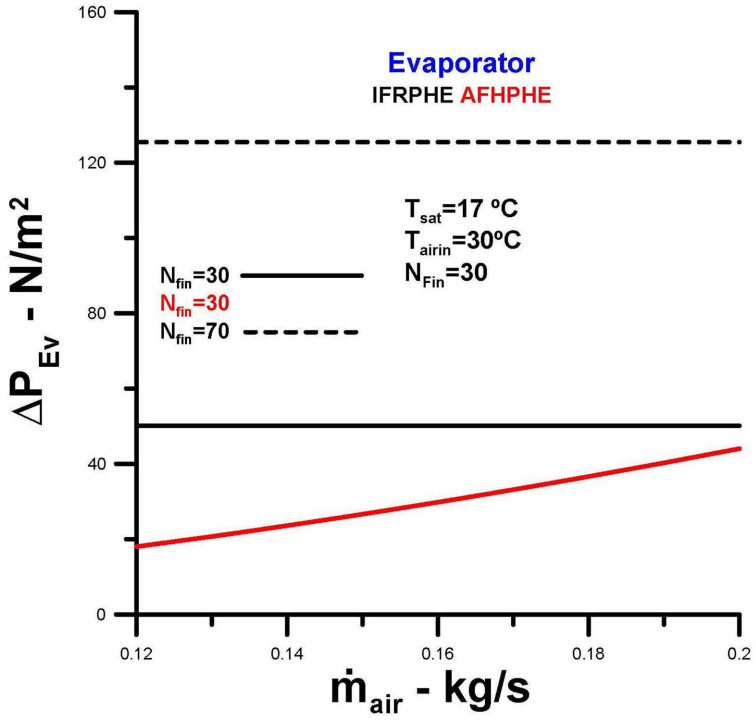

Figure 9. Pressure drops.

The Bejan number in the evaporator is represented in Figure 10. The Bejan number reflects the relative influence of viscous irreversibility on the overall performance of the heat exchanger. The weight of viscous irreversibilities in the IFHPHE is high and influences the low relative value of the Bejan number. In terms of viscous performance in the evaporator, the IFHPHE with 70 fins is poor, negating its excellent thermal performance and excluding it as an option. For 30 fins, the viscous performance of the IFHPHE is quite reasonable and outperforms most conventional heat exchangers. In the case of the AFHPHE, two simulations were implemented, simulating a pressure loss associated with the air outlet in the evaporator. Two pressure drop amplification factors shown in Figure 7 were added to Figure 8, 50% and 100% higher. When the 100% factor is imposed, there is an equality of viscous performance between the heat exchangers, for the maximum flow rate under analysis. For a 50% condition, the performance is exceptional.

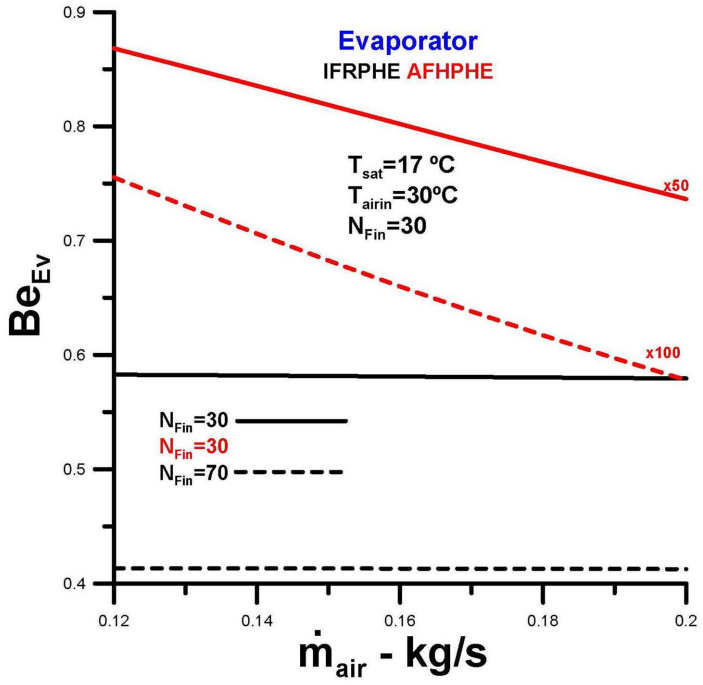

Figure 10. Bejan number.

3.2. Condenser

In this section, we begin the analysis and evaluation of the results obtained for the condenser region for both heat exchangers.

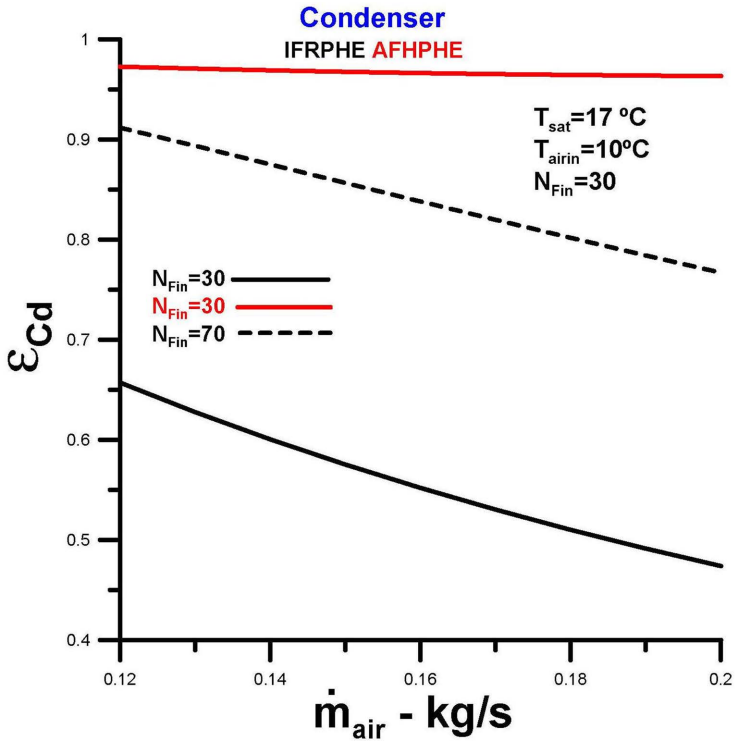

Figure 11. Effectiveness.

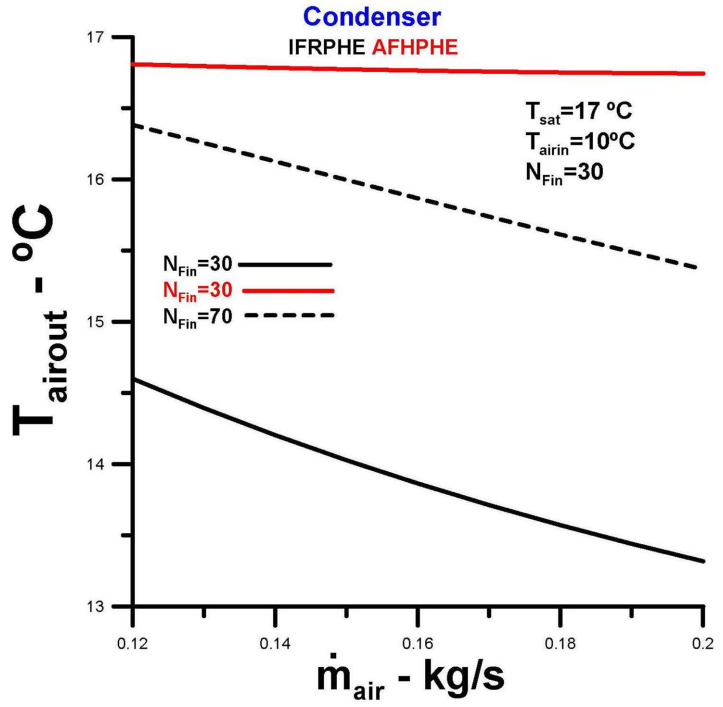

Figure 12. Temperature.

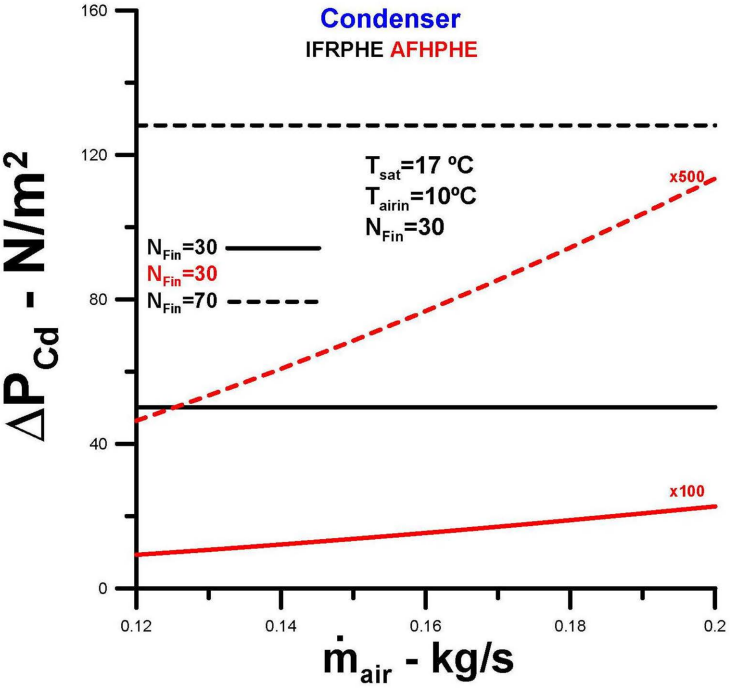

Figure 13. Pressure drops.

Only parameters relevant to objectively assessing the condenser's thermal and viscous performance were analyzed, as some overlap with those of the evaporator.

The effectiveness of the condenser is represented in Figure 11. The effectiveness of the AFHPHE is exceptional for 30 fins, due to its larger heat exchange area.

Superior thermal performance, compared to the evaporator, is achieved due to the counterflow arrangement. The effectiveness of the IFHPHE remains in a range of 0.45 to 0.66, for 30 fins. In the case of 70 fins for the IFHPHE, the efficiencies are similar, with lower performance for higher flow rates. These results, as previously evidenced, are crucial for the overall performance analysis of the heat exchangers.

Figure 12 reflects the results obtained for thermal effectiveness, with temperatures close to the saturation temperature of the working fluid in the case of the IFHPHE with 30 fins, across the entire flow rate range analyzed. The temperatures obtained for the IFHPHE are significantly below the saturation temperature of the working fluid for 30 fins, decreasing for higher flow rates. For 70 fins, the temperatures approach the saturation temperature of the working fluid for low flow rates and decrease with increasing flow rate.

Figure 13 presents the result of the pressure drop in the condenser. The results obtained reflect what has already been discussed for the evaporator, with a slight drop compared to the IFHPHE, since the evaporator length is twice the length of the condenser. A 100x simulation of the pressure drop in the tubes and shell of the heat exchanger shows that the pressure drop results are close to the pressure drop of the IFHPHE with 70 fins and maximum flow rate.

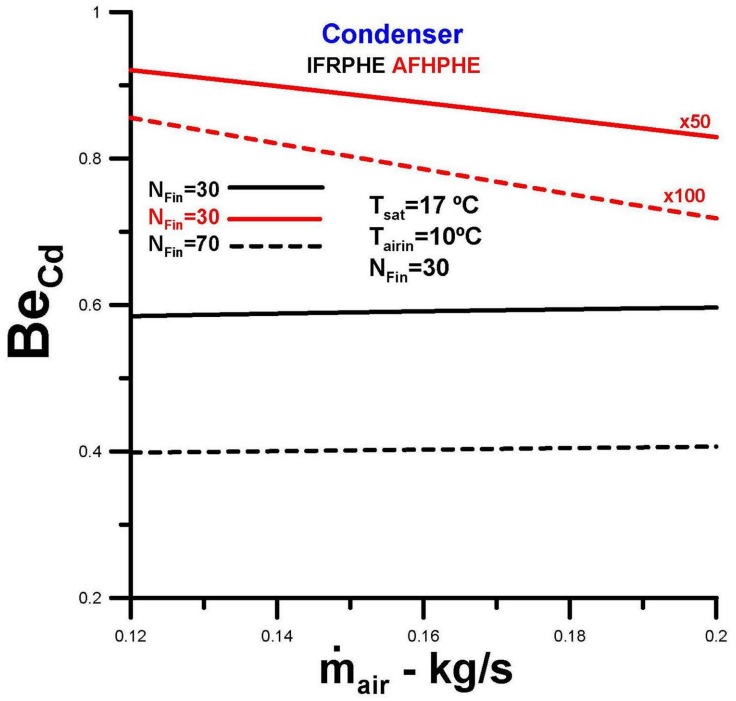

Figure 14. Bejan number.

The Bejan number in the evaporator is represented in Figure 14. The results obtained demonstrate a superior overall performance for the AFHPHE compared to the IFHPHE. The performance of the IFHPHE for 70 fins is equal to 40% of the maximum possible performance. Considering the pressure loss value, this result is significant and reflects the exceptional superiority of AFHPHE.

3.3. FHPHE

In this section, we present results related to the overall performance of heat exchangers.

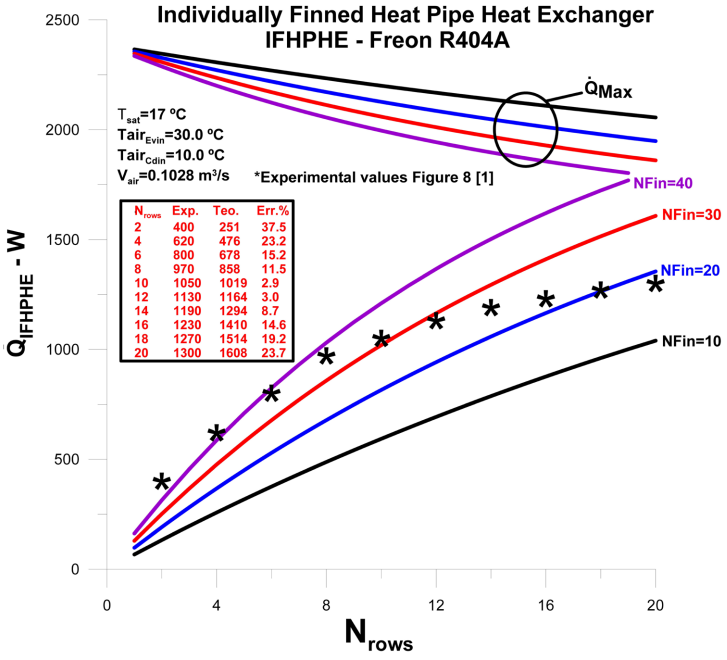

Figure 15. Theoretical versus experimental effectiveness [7].

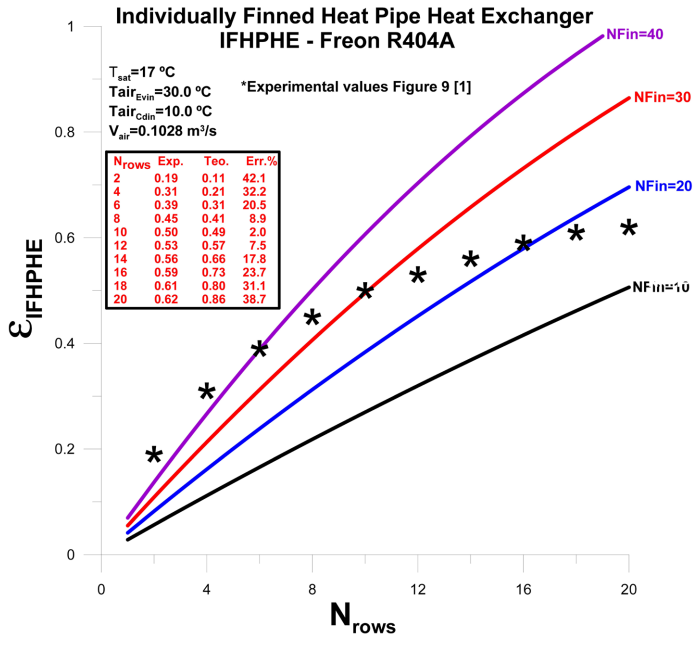

Figure 16. Theoretical and experimental heat transfer rate [7].

Figure 15 presents theoretical and experimental results for thermal effectiveness obtained for IFHPHE and presented through reference [7]. The results are

valid for the lowest air flow rate, approximately equal to 0.12 kg/s.

Figure 16 presents theoretical and experimental results obtained for heat transfer rate obtained for IFHPHE and reported through reference [7]. The results are valid for the lowest air flow rate, approximately equal to 0.12 kg/s.

The results for pressure loss presented in Figure 17 were reported in reference [7]. This is a theoretical experimental comparison for the IFHPHE, considering the variation in the number of tubes and the number of fins, for the lowest flow rate, equal to 0.12 kg/s. The experimental results for 30 fins coincide with the simulated results and demonstrate the consistency of the model developed for the IFHPHE.

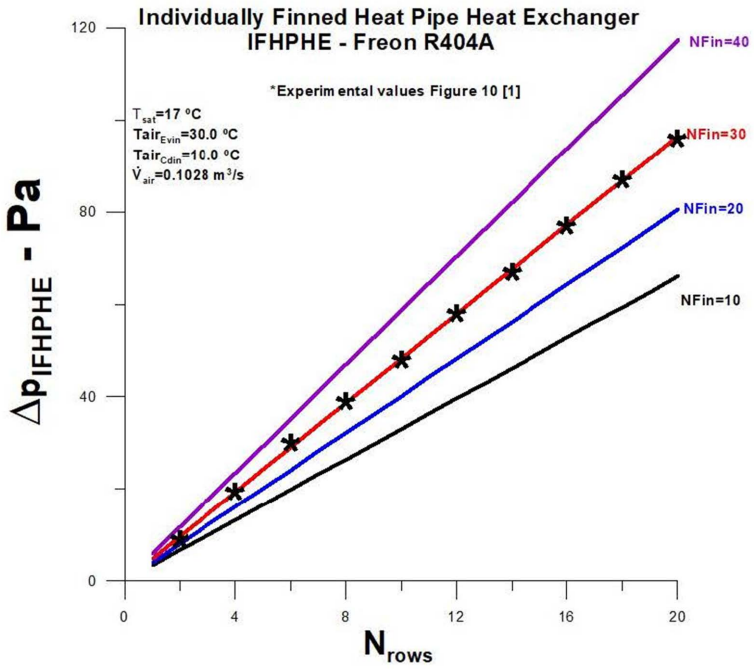

Figure 17. Pressure drops in the IFHPHE in relation to the number of fins [7].

Figure 18 presents the result for the overall effectiveness of both heat exchangers analyzed. The thermal performance of the AFHPHE is significantly superior to that obtained for the IFHPHE, for 30 fins, across the entire flow range. The thermal performance of the IFHPHE with 70 fins is slightly superior to that of the AFHPHE, across the entire flow range.

Figure 19 presents results reflecting the overall performance of the heat exchangers, using the Bejan number. The overall performance of the AFHPHE is superior across the entire flow range when the pressure drop corresponds to 50 times the pressure drop in the heat pipes and the shell of the heat exchanger, for the entire flow range and with several fins equal to 30. For a drop corresponding to 100 times the drop in the heat pipes, the performance is superior for low flow rates and slightly inferior for high flow rates. When the number of fins corresponds to 70 in the IFHPHE, the overall performance is very low, not justifying the configuration.

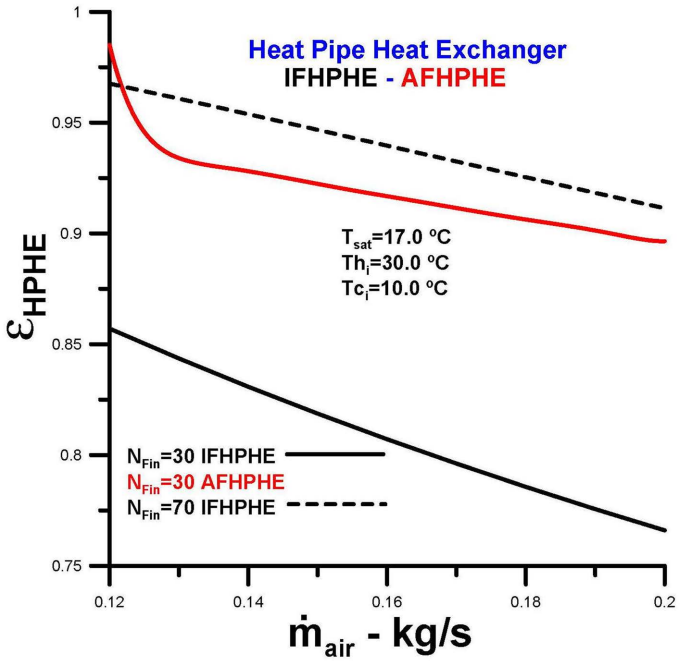

Figure 18. Overall thermal effectiveness for heat exchangers.

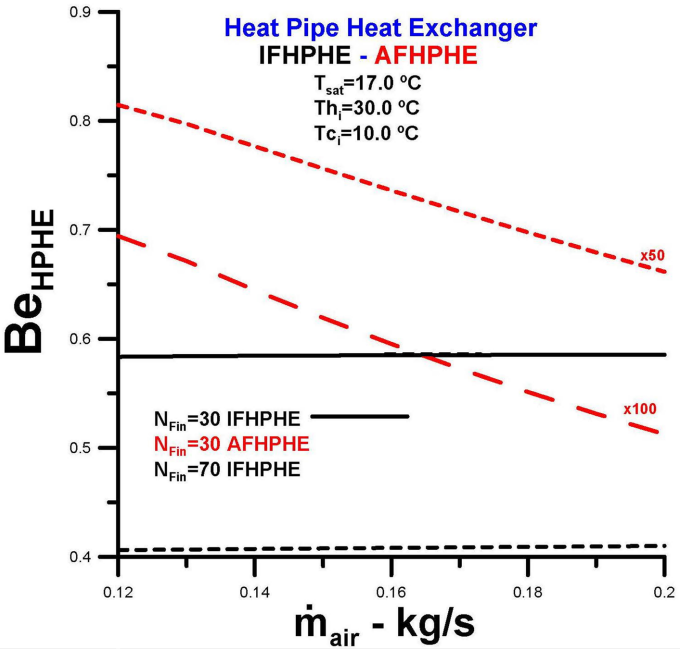

Figure 19. Bejan number for heat exchangers.

Considerations regarding pressure losses at the air outlets in the evaporator and condenser for the AFHPHE must be explicitly stated in this context, since they were imposed during the simulations, despite being realistic and oversized in relation to the heat exchanger design. These constraints were necessary during the simulation phase because the prototype's outlet design is still in the theoretical and experimental design phase, seeking the lowest possible viscous dissipation.

4. Conclusions

Comparisons are made between two finned tube heat exchangers: an individually finned tube heat exchanger (IFHPHE) and an axially finned tube heat exchanger (AFHPHE). The comparisons are made locally in the evaporator and condenser, and globally in the heat exchanger.

The fixed parameters used in the comparisons were the mass flow rates of air in the shell, varying from 0.12 kg/s to 0.20 kg/s, the temperature of the working fluid (R404a) $T_{sat} = 17.0^{\circ}\text{C}$, and the number of fins per heat pipe, equal to 30 fins (possibly 70 fins in the IFHPHE, for analysis purposes).

The quantities obtained in the theoretical analysis were velocities, Nusselt numbers, number of thermal units (NTU), thermal effectiveness, outlet temperatures, pressure losses, and Bejan numbers.

The results demonstrate that the heat exchange in the two heat exchangers is high and very close when the number of fins is kept at 30. When 70 fins are imposed for the IFHPHE, the thermal performance is higher than the performance of the AFHPHE for 30 fins and approaches the maximum possible.

Regarding pressure loss, the results presented show significantly different values for the heat exchangers. The pressure losses in the IFHPHE are higher than those obtained for the AFHPHE, and in the case of 70 fins, the difference is extremely high. These differences are justified by the design of the IFHPHE, which features crossflow and a staggered configuration for the tube rows, with a much larger air frontal area compared to the AFHPHE.

When analyzing Bejan's figures, which include thermal and viscous performance, the comparisons are very favorable for AFHPHE, with high thermal performance and a relatively low viscous effect compared to IFHPHE. With 30 fins per heat pipe, IFHPHE surpasses most standard heat exchangers. In the case of 70 fins for IFHPHE, despite the extremely high thermal performance, the cost-benefit ratio is not satisfactory, and its implementation should be discarded.

The prototype represented in **Figure 2** is not feasible, since four air outlets are impractical, despite being a diametrically homogeneous and aesthetically very well-conceived design for the AFHPHE.

Through the comparisons carried out, the superior overall performance of the AFTHE is demonstrated. However, the ideal configuration for the heat exchanger needs to be finalized so that the conclusions presented can be experimentally validated.

Conflicts of Interest

The authors declare no conflicts of interest regarding the publication of this paper.

References

[1] Górecki, G., Łęcki, M., Gutkowski, A.N., Andrzejewski, D., Warwas, B., Kowalczyk, M., *et al.* (2021) Experimental and Numerical Study of Heat Pipe Heat Exchanger with Individually Finned Heat Pipes. *Energies*, **14**, Article 5317. https://doi.org/10.3390/en14175317

[2] Nogueira, É., Diniz, F.D.S.F., Felix, R. and Tavares, E.L.D.O. (2025) Evaluation of the Theoretical Design and Mathematical Modeling for Determination of Thermal and Viscous Irreversibilities in Axially Finned Two-Phase Closed Thermosyphon Heat Exchanger. *Journal of Materials Science and Chemical Engineering*, **13**, 48-78. https://doi.org/10.4236/msce.2025.1311005

[3] Putra, N., Anggoro, T. and Winarta, A. (2017) Experimental Study of Heat Pipe Heat Exchanger in Hospital HVAC System for Energy Conservation. *International Journal on Advanced Science, Engineering and Information Technology*, **7**, Article 871. https://doi.org/10.18517/ijaseit.7.3.2135

[4] Sukarno, R., Putra, N., Hakim, I.I., Rachman, F.F. and Mahlia, T.M.I. (2021) Multi-Stage Heat-Pipe Heat Exchanger for Improving Energy Efficiency of the HVAC System in a Hospital Operating Room. *International Journal of Low-Carbon Technologies*, **16**, 259-267. https://doi.org/10.1093/ijlct/ctaa048

[5] Ibnu Hakim, I., Sukarno, R. and Putra, N. (2021) Utilization of U-Shaped Finned Heat Pipe Heat Exchanger in Energy-Efficient HVAC Systems. *Thermal Science and Engineering Progress*, **25**, Article 100984. https://doi.org/10.1016/j.tsep.2021.100984

[6] Nogueira, É. (2023) Theoretical Thermal Performance of Cross-Flow Finned Heat Pipe Heat Exchanger Used for Air Conditioning in Surgery Rooms. *Mechanical Engineering Advances*, **1**, Article 131. https://doi.org/10.59400/mea.v1i1.131

[7] Nogueira, É. (2023) Thermal and Viscous Irreversibilities in the Heat Exchanger of Individually Finned Heat Pipes Using Freon R404A as the Working Fluid. *Mechanical Engineering Advances*, **1**, Article 132. https://doi.org/10.59400/mea.v1i1.132

[8] Nogueira, É. (2025) Heat Exchangers: Analytical Modeling and Applications. Editora Dialética.

[9] Fakheri, A. (2007) Heat Exchanger Efficiency. *Journal of Heat Transfer*, **129**, 1268-1276. https://doi.org/10.1115/1.2739620

[10] Hameed, M.S., Khan, A.R. and Mahdi, A.A. (2013) Modeling a General Equation for Pool Boiling Heat Transfer. *Advances in Chemical Engineering and Science*, **3**, 294-303. https://doi.org/10.4236/aces.2013.34037

[11] Rohsenow, W.M. (1951) A Method of Correlating Heat Transfer Data for Surface Boiling of Liquids. Technical Report No. 5. The Office Naval Research Contract N5ori-07827, Massachusetts Institute of Technology.

[12] Pioro, I.L., Rohsenow, W. and Doerffer, S.S. (2004) Nucleate Pool-Boiling Heat Transfer. II: Assessment of Prediction Methods. *International Journal of Heat and Mass Transfer*, **47**, 5045-5057. https://doi.org/10.1016/j.ijheatmasstransfer.2004.06.020

[13] Nogueira, E. (2020) Analytical and Numerical Methods with Engineering Applications in Heat Transmission and Fluid Mechanics. Appris Editora.

[14] Zimparov, V.D., Angelov, M.S. and Hristov, J.Y. (2021) Critical Review of the Definitions of the Bejan Number—First Law of Thermodynamics. *International Communications in Heat and Mass Transfer*, **124**, Article 105113. https://doi.org/10.1016/j.icheatmasstransfer.2021.105113

Nomenclature

$Asec$: cross-section area, [m^2]

Atr : heat transfer area, [m^2]

Cp : specific heat, [$\frac{J}{kg\,K}$]

C : thermal capacity, [$\frac{W}{K}$]

C_{min} : minimum thermal capacity, [$\frac{W}{K}$]

$C^* = \frac{C_{min}}{C_{max}}$

D_h : hydraulic diameter, [m]

Fa : fin analogy

h : coefficient of heat convection, [$\frac{W}{m^2\,K}$]

k : thermal conductivity, [$\frac{W}{m\,K}$]

K : Kelvin

k_W : thermal conductivity of the tube, [$\frac{W}{m\,K}$]

k_{Fin} : thermal conductivity of the fin, [$\frac{W}{m\,K}$]

L : vertical or horizontal length, [m]

$\dot{m}_{air}$: mass flow rate of the air, [$\frac{kg}{s}$]

N_{Fin} : number of fins

Nu : Nusselt number

Pr : Prandtl number

$\dot{Q}$: actual heat transfer rate, [W]

$\dot{Q}_{max}$: maximum heat transfer rate, [W]

Re : Reynolds number

T: temperatures, [˚C]

Uo : global heat transfer coefficient, [$\frac{W}{m^2\,K}$]

Subscripts

boil: ebulição

Cd: Condenser

Cond: Condenser

effect: effective

Ev: Evaporator

ext: external

HP: heat pipe

H: horizontal
in: inlet
int: internal
out: outlet
sat: saturation

Greek Symbols

α : thermal diffusivity, $[\frac{m^2}{s}]$

β: the relationship between areas

ρ: density of the fluid, $[\frac{kg}{m^3}]$

μ: dynamic viscosity of fluid, $[\frac{kg}{ms}]$

ν : kinematic viscosity of the cold fluid, $[\frac{m^2}{s}]$

ε_T : thermal effectiveness

η_T : thermal efficiency

ΔT : a difference of temperatures, [˚C]

Acronyms

FHPHE: Finned heat pipe heat exchanger
Ev: Evaporators
Cd: Condenser
NHP: Number of Heat Pipes
NFin: Number of Fins
Nrows: Number of rows
NTU: number of thermal units